https://jurnaleeccis.ub.ac.id/
e-ISSN(Online): 2460-8122

Jurnal EECCIS Vol. 17, No. 2, Agustus 2023
pp 41-52

Study of Permanent Magnet Synchronous Motor with LQG Controller and *Observer* on the Hydraulic Pump System

Paulus Setiawan[1], Linda Meilani[2], Denny Dermawan[3], Freddy Kurniawan[4], Okto Dinaryanto[5]
[1,2,3,4] Program Studi Teknik Elektro, Institut Teknologi Dirgantara Adisutjito, Yogyakarta
[5]Program Studi Teknik Mesin, Institut Teknologi Dirgantara Adisutjito, Yogyakarta
Email: paulussetiawan@stta.ac.id[*] , meilanielinda789@gmail.com, dennydermawanstta@gmail.com, freddykurniawan@itda.ac.id, okto.dinaryanto@itda.ac.id

***Abstract*—In today's aircraft industry, the flight control system and landing gear system cannot be separated from the role of the hydraulic technology system. As the prime mover of the hydraulic pump or actuator hydraulic system, a permanent magnet synchronous motor (PMSM) is used. This PMSM is a substitute for the role of conventional combustion engines which PMSM is considered to have several advantages in increasing performance and efficiency. This research will develop a system to find parameter values for Linear Quadratic Gaussian (LQG) controllers in a hydraulic pump system that is installed as a load from PMSM, and then observe and analyze the performance of the response of the synchronous motor system, namely in the form of changes in rotor rotation speed, torque electric power, and stator current on the q-axis. From the results of the research on the characteristics of the PMSM implemented in the hydraulic pump system, it can be seen that the LQG controller is more optimal when compared to the observer controller. The LQG controller is known to have a faster transient response, which is indicated by the value of the settling time improvement at no load, namely 116.67% for the observer controller and 364.705% without the controller. Then when the synchronous motor serves the nominal load, the rotational speed of the rotor produced in steady state becomes 8.29% faster than the observer controller and 74.49% without the controller. The rotational speed of this rotor affects the time needed by the actuator to extend and retract motion.**

Keywords—Permanent Magnet Synchronous Motor, hydraulic pump, Linear Quadratic Gaussian, obserever

I. Introduction

PMSM is a device that is designed using a permanent magnet embedded in a steel material rotor which functions to produce a constant magnetic field. This type of permanent magnet synchronous motor is one of the best choices for a wide range of industrial applications in rotor speed control systems. The stator winding is a winding connected to an alternating power source to produce a rotating magnetic field. Then when the rotor speed reaches synchronous speed with the stator rotating speed, the rotor poles will lock the rotating stator magnetic field. This permanent magnet synchronous motor is similar to a brushless DC motor. Some of the advantages of this permanent magnet synchronous motor are low torque ripple, high efficiency, high power density, low heating rate, and low maintenance costs. But besides having advantages, there are also disadvantages such as the level of complex control systems, both from scalar control and vector control. In vector control, changes in stator current or changes in rotor speed can be used as feedback in a plant system.

While on the other hand, the hydraulic actuator is a power transmission system device that is most commonly used, which requires a high level of power density, robustness, reliability, high temperature operation, light weight, and low volume. However, if it is still driven by conventional hydraulic engines and Electro-Hydraulic (EH) actuators, these conventional hydraulic machines still have fundamental limitations, namely limitations in achieving high efficiency due to excessive throttle pressure loss and high heat generation in the servovalve.

II. Related Research

Electro-Mechanical (EM) and Electro-Hydrostatic (EHA) actuators were introduced to replace conventional actuators. These EM and EHA actuators have the simplest structure but provide a high level of efficiency. This EHA uses a variable speed electric power system to drive a hydraulic pump where the role of the servovalve is then removed. Overall efficiency in EHA system is higher than EH [1].

Then research that has analyzed PMSM in controlling hydraulic pumps as actuator drives in vehicle steering, was carried out using the Field Oriented Control (FOC) method. FOC provides wider speed settings and smoother characteristics, but controlling the adjustment is quite complicated. The main objectives of this research are determination of control values for actuators controlled by hydraulic pumps and analysis of system behavior in different applications. The results of this study require a larger current power supply, more complex frequency converter settings, but can achieve a higher level of accuracy and can reduce the ripple value of the motor torque [2].

Research that has evaluated the energy efficiency of electro-hydraulic forklifts can be significantly improved by using direct control of a hydraulic pump based on PMSM to control fork position without valve control. By selecting the appropriate motor power, the total system efficiency can be increased by even 20% units under different operating conditions and also the energy saving ratio can be increased by 5% to 9% per unit [3].

The study compared the stability gain of the two controllers applied to the electro-hydraulic steering system, namely the LQG controller and the H-infinity controller. The two controllers are synthesized into the modeling of the state-space system which is obtained by identifying the plant. In order to investigate the strengthening of the stability of the closed loop system up to 30%, the uncertainty parameter is entered into matrix B of the model which describes the observed hysteresis of the electrohydraulic actuator. The H-infinity controller achieves a smaller gain value than the LQG controller in a limited variation in the characteristic model [4].

Research that has analyzed the optimal control system with vector control for PMSM and then compared the results with conventional vector control has achieved good results. The interim results at the time of the previous measurement were that there was a lot of noise and the LQG methodology used to filter out the noise level was not maximized. The results of optimal vector control on noise (without filter) and filtered vector optimal control compared to one another. Then the PMSM nonlinear results and the presence of an inverter in the control circuit cause the system to become more nonlinear and time-invariant. By deriving the equations and model averaging, then the system is converted to nonlinear time invariant and then the time invariant is converted to a linear system of linearized equations to the averaging model. The simulation results show that the performance and resistance to noise of the control system can be improved [5].

Motor speed control by forming a transient speed response mounted on the PMSM surface is achieved by using the linearized feedback method and the development of a high-gain observer. To improve the feedback linearization performance, a high-gain observer is used to estimate the speed of the two motors and also to estimate the disturbances that occur in the system. The observer is designed based on the derivation of the PMSM equation model, which is realized through the application of a single perturbation theory to the motor. Motor parameters are assumed to be indeterminate and only assume readings of motor nominal value. Torsional external loads are also assumed to be unknown and time-varying, but limited. Then the stability value of the output feedback system is analyzed. The experimental results confirm the performance and durability of the designed controller and compare it with the proportional integral (PI) speed controller in stages [6].

From some of the research reference descriptions above that have been carried out including regarding EHA, PMSM, PI controllers, LQG controllers, and H-infinity controllers, the novelty of this research is to find parameter values that show the characteristics of a system for LQG controllers in hydraulic systems. pump which is objectively as a load from PMSM, and then compares the results of the response if using an observer controller.

III. Research Methodology

This research will develop research that has been done by (Lee, 2017) [1] in Figure 1, with the first research step in the form of modeling the PMSM mathematical equation and calculating the parameters on the motor, then modeling the observer controller, then modeling the LQG controller. After all the mathematical model equations have been known and all the controlling parameters on the motor have been calculated, the next research step is to observe and analyze the performance of the response of the synchronous motor system, namely in the form of changes in rotor rotation speed, electric power torque, and stator current on the axes q.

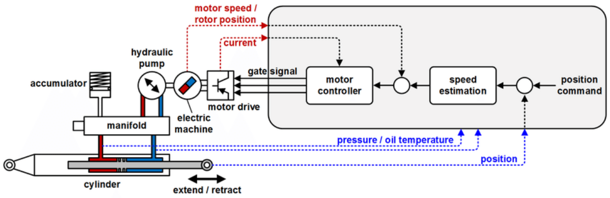

Figure 1. Electro-Hydrostatic Actuator system schematic (EHA) [1]

A. PMSM

The design of the PMSM speed controller is important in terms of transient characteristics and steady state characteristics. Integral proportional amplification is suitable for application in various industries so it is very important to note. The selection of gain and time constants for motor speed control uses the optimal system principle which is directly assumed if the stator current on the d-axis is zero. In the presence of the d-axis of the stator current, the currents of the d-axis and the q-axis are interrelated as parameters for calculating torque loads.

Assuming that $i_{ds}^r = 0$, then the system becomes linear as in a DC motor with constant separate gain. From this assumption, the derivation of the block diagram on current is like an approach to deceleration, and the derivation of speed controllers with optimal systems so that they become identical to DC motors, such as the procedure for designing speed controllers for induction motors using vector control techniques.

Derivation of the equation on the block diagram and the equation of the motor voltage on the q-axis with the d-axis current at the start becomes

$$v_{qs}^r = (R_s + L_q p) i_{qs}^r + \omega_r \lambda_{af} \tag{1}$$

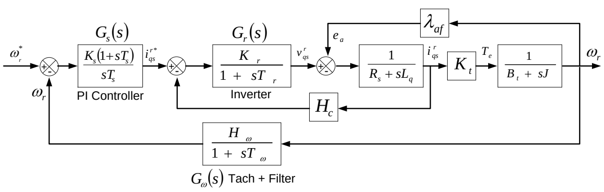

Figure 2. PMSM speed controller block diagram [8]

and the electromechanical equation of the motor is

$$\frac{P}{2}\left(T_e - T_l\right) = Jp\omega_r + B_1\omega_r \quad (2)$$

where for the electromagnetic torque equation is

$$T_e = \frac{3}{2}.\frac{P}{2}\lambda_{af} i_{qs}^r \quad (3)$$

and if there is a load that is assumed to be a frictional force, then $T_l = B_l\omega_m$ (4)

where the substitution electromechanical equation is given as

$$\left(Jp + B_t\right)\omega_r = \left[\frac{3}{2}\left(\frac{p}{2}\right)^2 .\lambda_{af}\right] i_{qs}^r = K_t . i_{qs}^r \quad (5)$$

where

$$B_t = \frac{P}{2}B_l + B_l \quad (6)$$

$$K_t = \frac{3}{2}\left(\frac{P}{2}\right)^2 .\lambda_{af} \quad (7)$$

In equations (1) and (5), when combined into the block diagram the feedback along with the current and the increase in rotor speed is shown in Figure 2. The inverter modeled is as a gain together with a lag time constant, namely

$$G_r(s) = \frac{K_r}{1 + sT_r} \quad (8)$$

where $K_r = 0.65\frac{V_{dc}}{V_{cm}}$ and $T_r = \frac{1}{2f_c}$ (9)

The emf induction as the scope of the flux linkage e_a is

$$e_a = \lambda_{af}\,\omega_r(V) \quad (10)$$

Multiply the emf induction loop with the current loop on the q-axis and this process can be simplified by changing the node for the emf induction loop from velocity to current output point.

$$\frac{i_{qs}^r(s)}{i_{qs}^{r*}(s)} = \frac{K_r K_a\left(1 + sT_m\right)}{H_c K_a K_r\left(1 + sT_m\right) + \left(1 + sT_r\right)\left\{K_a K_b + \left(1 + sT_a\right)\left(1 + sT_m\right)\right\}} \quad (11)$$

where

$$K_a = \frac{1}{R_s}; T_a\frac{L_q}{R_s}; K_m\frac{1}{B_t}; T_m = \frac{J}{B_t}; K_b = K_t K_m \lambda_{af} \quad (12)$$

By using an approximate value that is close to the multiplication of the frequencies around it, then:

$$1 + sT_r \cong 1 \text{ then } 1 + sT_m \cong sT_m \quad (13)$$

$$\left(1 + sT_a\right)\left(a + sT_r\right) \cong 1 + s\left(T_a + T_r\right) \cong 1 + sT_{ar} \quad (14)$$

where $T_{ar} = T_a + T_r$ (15)

together with the transfer function in the current loop is estimated as

$$\frac{i_{qs}^r(s)}{i_{qs}^{r*}(s)} \cong \frac{\left(K_a K_r T_m\right)s}{K_a K_b + \left(T_m + K_a K_r T_m H_c\right)s + \left(T_m T_{ar}\right)s^2}$$

$$\cong \left(\frac{T_m K_r}{K_b}\right)\frac{s}{\left(1 + sT_1\right)\left(1 + sT_2\right)} \quad (16)$$

Where can this equation be found $T_1 < T_2 < T_m$ and so, on a more precise approximation that, $\left(1 + sT_2\right) \cong sT_2$. The approximate transfer function in the current loop is as follows

$$\frac{i_{qs}^r(s)}{i_{qs}^{r*}(s)} \cong \frac{K_i}{\left(1 + sT_i\right)} \quad (17)$$

where $K_i = \frac{T_m K_r}{T_2 K_b}$ dan $T_i = T_1$ (18)

Then the equation approach to frequency multiplication is

$$\left(1 + sT_m\right) \cong sT_m \quad (19)$$

$$\left(1 + sT_i\right)\left(1 + sT_\omega\right) \cong 1 + sT\omega wi \quad (20)$$

$$1 + sT_\omega \cong 1 \text{ where } T_{\omega i} = T_\omega + T_i \quad (21)$$

The approach for the transfer function in the rotor speed loop can be simplified as shown in Figure 2., and written as

$$GH(s) \cong \frac{K_i K_m K_t H_\omega}{T_m}\cdot\frac{K_s}{T_s}\cdot\frac{\left(1 + sT_s\right)}{S^2\left(1 + sT_{\omega i}\right)} \quad (22)$$

Which the closed feed of the velocity transfer function can be written as

$$\frac{\omega_r(s)}{\omega_r^*(s)} \cong \frac{1}{H_\omega}\left\{\frac{K_g\,\frac{K_s}{T_s}\left(1 + sT_s\right)}{s^3 T_{\omega i} + s^2 + K_g\,\frac{K_s}{T_s}\left(1 + sT_s\right)}\right\} \quad (23)$$

where

$$K_g = \frac{K_i K_m K_t H_\omega}{T_m} \quad (24)$$

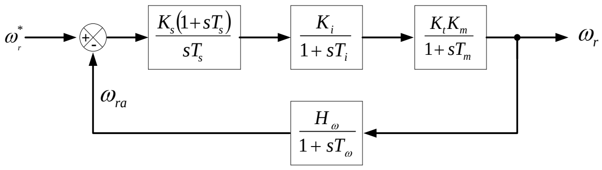

Figure 3. Simplification of the rotor speed controller [8]

The transfer function equation is in the symmetrical optimal function with a damping ratio of 0.707, giving the transfer function in the rotor speed loop as (Figure 3.)

$$\frac{\omega_r(s)}{\omega_r^*(s)} \cong \frac{1}{H_\omega}\cdot\frac{\left(1 + sT_s\right)}{1 + \left(T_s\right)s + \left(\frac{3}{8}T_s^2\right)s^2 + \left(\frac{1}{16}T_s^3\right)s^3} \quad (25)$$

In equations (23) and (25), solving the equation coefficients and constant values will produce the time constant values and the rotor speed control constant values as

$$T_s = 6T_{\omega i} \text{ and } K_s = \frac{4}{9K_g T_{\omega i}} \quad (26)$$

B. *Full Order Observer State Feedback*

By observing a system in a state

$$\dot{x} = Ax + Bu$$
$$y = Cx \quad (27)$$

Then choose the control system form

$$u = \left(r - Kx\right) \quad (28)$$

In equation (28), K is referring to the state feedback reinforcement matrix and r_t .is the vector aimed at the state space variables. The block diagram of state space variables show Equations (27) and (28). By substituting in equation (28) into equation (27) it will be obtained

$$\dot{x} = Ax + B(r - Kx) \tag{29}$$

The result matrix $(A - BK)$ is a matrix system with a closed loop as in equation (29). For a system described from equation (27), the characteristics of the equation are

$$|(sI - A)| = 0 \tag{30}$$

The roots in equation (30) are the eigenvalues in open-loop polishing. The characteristic equation for closed loop system becomes

$$|(sI - A + BK)| = 0 \tag{31}$$

The roots in equation (31) are the eigenvalues of the closed-loop poles.

In the system, the full-order state observer estimates all state variables. However, if several state variables have been measured, then it may only be needed to estimate some of state variabels, known as the reduced-order state observer. Some forms of mathematical modeling are used by all observers to produce estimates of $\hat{x}$ the actual state x vector. It is assumed to estimate the value $\hat{x}$ of a state vector is

$$\hat{x} = A\hat{x} + Bu + K_e\left(y - C\hat{x}\right) \tag{32}$$

where K_e is an observer gain matrix. If equation (32) is a subtraction of the previous equation and $\left(x - \hat{x}\right)$ is an error vector e, then

$$\dot{e} = (A - K_eC)e \tag{33}$$

next the equation for a full-order state observer is

$$\hat{x} = (A - K_eC)\hat{x} + Bu + K_e y \tag{34}$$

A dynamic behavior of an error vector depends on the eigenvalues as equation (33) . So that at every measurement of a system, these eigenvalues $(A - K_eC)$ should follow the response of the transient observer to be faster than the system itself, unless the effect of filtering is ignored.

The observer design problem is basically the same as the placing problem of pole regulator, and has the same technique to use, namely the direct comparison method. This method is $s = u_1, s = u_2, \ldots, s = u_n$ then

$$\begin{aligned}|sI - A + K_eC| &= (s - u_1)(s - u_2)\ldots(s - u_n)\\ &= s^n + \alpha_{n-1}s^{n-1} + \ldots + \alpha_1 s + \alpha_0\end{aligned} \tag{35}$$

A control system is implemented by using observer space variables

$$u = -K\hat{x} \tag{36}$$

If there is a difference between the actual value and the value of the observer space variable, it is

$$e(t) = x(t) - \hat{x}(t) \text{ then } \hat{x}(t) - e(t) \tag{37}$$

The combination of equations (32) and (34) will give the closed loop equation, namely

$$\begin{aligned}\dot{x} &= Ax - BK(x - e)\\ &= (A - BK)x + BK_e\end{aligned} \tag{38}$$

For the observer error equation from equation (33) is

$$\dot{e} = (A - K_eC)e \tag{39}$$

The combination of equations (38) and (39) gives

$$\begin{bmatrix}\dot{x}\\ \dot{e}\end{bmatrix} = \begin{bmatrix}A - BK & BK\\ 0 & A - B_eC\end{bmatrix}\begin{bmatrix}x\\ e\end{bmatrix} \tag{40}$$

Equation (40) describes closed loop dynamics in an observer feedback control system and the characteristics of the equation become

$$|sIA + BK||sI - A + K_eC| = 0 \tag{41}$$

Equation (41) shows that the desired closed-loop poles in the control system were not affected by the introduction of the state-observer. The roots of the equation from the pole-placement will dominate, because the observer uses a normal design for a faster response than the control system with full order observed state feedback as shown in Figure 3.

By substituting vector space $x(t)$ and $\hat{x}(t)$ of equations (36) and (37), the space equation of the closed loop system is

$$\dot{x} = Ax - BK\hat{x} \tag{42}$$

$$\begin{aligned}\hat{x} &= (A - K_eC)\hat{x} - BK\hat{x} + K_eCx\\ &= (A - K_eC - BK)\hat{x} + K_eCx\end{aligned} \tag{43}$$

so the equation of the closed-loop state space is (Fig. 4.)

$$\begin{bmatrix}\dot{x}\\ \hat{x}\end{bmatrix} = \begin{bmatrix}A & -BK\\ K_eC & A - K_eC - BK\end{bmatrix}\begin{bmatrix}x\\ \hat{x}\end{bmatrix} \tag{44}$$

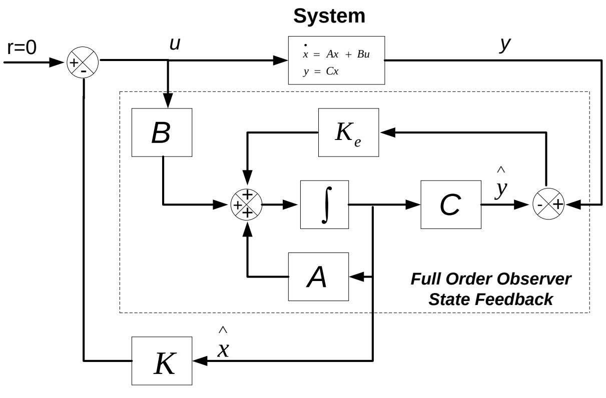

Figure 4. Full-order observer state feedback of control system [9]

C. *Linear Quadratic Regulator (LQR)*

The general problem of optimal control is to find the control μ which the system represented as follows

$$\dot{x} = g(x(t), \mu(t), t) \tag{45}$$

To follow the optimal path that minimizes the quadratic performance criterion

$$J = \int_{t_0}^{t_1} h(x(t), u(t), t)dt \tag{46}$$

Determination shape of the functional equation

$$f(x, t)\min_{u} \int_{t_0}^{t_1} h(x, u)dt \tag{47}$$

where during the time interval t_0 until t_1

$$f(x,t_0)= f(x(0))\ ;\ f(x,t_1)=0 \tag{48}$$

From equations (45) and (46), the Hamilton-Jacobi equation can be expressed as

$$\frac{df}{dt}=-\min_u\left[h(x,u)+\left(\frac{df}{dx}\right)^T g(x,u)\right] \tag{49}$$

In a linear form, the time invariant plant in equation (45) becomes $\dot{x}=Ax+Bu$, and if in equation (46) is the performance index of the quadratic value then

$$J=\int_{t_0}^{t_1}\left(x^TQx+u^TRu\right)dt \tag{50}$$

substitution of equation (50) into equation (49) becomes

$$\frac{df}{dt}=-\min_u\left[x^TQx+u^TRu+\left(\frac{df}{dx}\right)^T(Ax+Bu)\right] \tag{51}$$

Shows shape relationships $f(x,t)x^TPx$, where P is a square symmetric matrix then $\frac{df}{dt}=x^T\frac{d}{dt}Px$ and $\frac{df}{dx}=2Px$,then

$$\left[\frac{df}{dx}\right]^T=2x^TP \tag{52}$$

By entering equation (52) into (51),

$$x^T\frac{dP}{dt}x=-\min_u\left[x^TQx+u^TRu+2x^TP(Ax+Bu)\right] \tag{53}$$

from equation (53) to minimize the value of the matrix u,

$$\frac{d[df/dt]}{du}=2u^TR+2x^TPB=0 \tag{54}$$

Equation (54) can be simplified again to give the optimal control technique

$$u_{opt}=-R^{-1}B^TPx \text{ or } u_{opt}-Kx \tag{55}$$

where matrix K, $K=R^{-1}B^TP$. Then substitution of equation (55) into equation (53) can give the equation

$$x^TPx=-x^T\left(Q+2PA-PBR^{-1}B^TP\right)x \tag{56}$$

when $2x^TPAx=x^T\left(A^TP+PA\right)x$, then

$$\dot{P}=-PA-A^TP-Q+PBR^{-1}B^TP \tag{57}$$

Equation (57) known as matrix Riccati equations. The coefficient *P(t)* is found by integration in the past starting with the boundary condition $x^T(t1)P(t1)x(t1)=0$. Kalman show that integration in time inversion has occurred, so that the solution of *P(t)* converges to a constant value. If it T_1 is infinite, or it is far from T_0, then the matrix of the Riccati equations can be reduced to a set of simultaneous equations

$$PA+A^TP+Q-PBR^{-1}B^TP=0 \tag{58}$$

Equations (57) and (58) are answers in the continuous form of the Riccati matrix equation.

D. LQG

In conventional LQG control, it is assumed that the dynamics of a plant model is linear with known parameter constants, and measurements of noise or disturbance signals (noise processes) are stochastic with statistical properties that can also be known beforehand. This means, a plant model has similarities

$$\dot{x}=Ax+Bu+wd \tag{59}$$

$$y=Cx+Du+wn \tag{60}$$

When matrix D is 0, *wn* and *wd* are input noise measurements and noise such as process noise, i.e. zero-mean Gaussian stochastic processes are uncorrelated with constant power spectral density matrices *V* and *W*. Then *wn* and *wd* are noise processes with covariance functions.

$$E\left[w_d(t)w_d(\tau)^T\right]=W\delta(t-\tau) \tag{61}$$

$$E\left[w_n(t)w_n(\tau)^T\right]=V\delta(t-\tau)\text{ , dan} \tag{62}$$

$$E\left[w_d(t)w_n(\tau)^T\right]=0, E\left[w_n(t)w_d(\tau)^T\right]=0 \tag{63}$$

Where *E* is an approximate matrix value and $\delta(t-\tau)^T$ is a delta function.

The problem of an LQG control is to determine the optimal control *u(t)* so that

$$J=E\left[\lim_{T\to 0}\frac{1}{T}\int_0^T\left(x^TQx+u^TRu\right)dt\right] \tag{64}$$

where *R* and *Q* are the selected weighting matrix constants so that $R=R^T>0$ and $Q=Q^T\geq 0$. The name LQG arose from the use of linear models, quadratic integral function values, and white noise Gaussian processes to model noise and disturbance signals.

The solution of the LQG problem is known as the Separation Theorem or the Equivalence of Certainty Principle. This first consists of determining the optimal control for the determination of the linear quadratic regulator (LQR) problem: that is, the above LQG problem without wn and wd. The problem solution can be written in terms of a simple feedback law.

$$u(t)=-K_rx(t) \tag{65}$$

where K_r is a matrix constant that is easy to calculate and obviously independent of *W* and *V* , that is, as a statistical property of a plant's noise. The next step is to find an optimal $\hat{x}$ estimate of state *x*, so that $E\left[\left(x-\hat{x}\right)^T\left(x-\hat{x}\right)\right]$ it can be minimized. This optimal state estimate is given by the Kalman filter and is independent of the values of R and Q. The required solution to the LQG problem, then found by replacing *x* with $\hat{x}$, is given to the function $u(t)=-K_r\hat{x}(t)$. Therefore the LQG problem and its solutions can be separated into two different parts as shown in Figure 3.

The LQR problem in optimal state feedback, where all states are known, there is a problem of determining the initial value that is given to the system $\dot{x}=Ax+Bu$

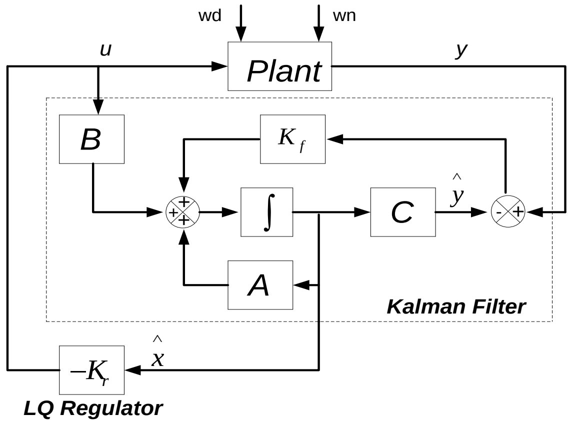

Figure 5. LQG controller and *noisy plant* [10]

with a non-zero initial state *x(0)*, to determine the input signal *u(t)* which brings the system to a state of zero *(x = 0)* optimally, namely by minimizing the value of losses

$$J_r = \int_0^{\infty} \left(x(t)^T Qx(t) + u(t)^T Ru(t) \right) dt \tag{66}$$

An optimal solution (for each initial state) is $u(t) = -K_r x(t)$, where

$$K_r = R^{-1} B^T X \tag{67}$$

$X = X^T \geq 0$ is a unique positive-semidefinite solution of the Riccati algebraic equation, ie

$$A^T X + XA - XBR^{-1} B^T X + Q = 0 \tag{68}$$

The Kalman filter as shown in Figure 5 has a structure of an ordinary-state-estimator or observer with

$$\dot{\hat{x}} = A\hat{x} + Bu + K_f \left(y - C\hat{x} \right) \tag{69}$$

The optimal choice of matrix K_f, where for the minimum value of $E\left\{ \left[x - \hat{x} \right]^T \left[x - \hat{x} \right] \right\}$, is given by

$$K_f = YC^T V^{-1} \tag{70}$$

where $Y = Y^T \geq 0$ is the unique positive-semidefinite solution of the Riccati algebraic equation. LQG is a combination of optimal state estimation with optimal state feedback.

$$YA^T + AY - YC^T V^{-1} CY + W = 0 \tag{71}$$

$$K_{LQG}(s) \stackrel{s}{=} \begin{bmatrix} A - BK_r - K_f C & K_f \\ -K_r & 0 \end{bmatrix}$$

$$= \begin{bmatrix} A - BR^{-1} B^T X - YC^T V^{-1} C & YC^T V^{-1} \\ -R^{-1} B^T X & 0 \end{bmatrix} \tag{72}$$

IV. Hasil dan Analisis

The data used in this PMSM research are data used by research [11]:

A. Calculating PMSM Parameters

To calculate and determine the constants of the parameters in the PMSM motor circuit, start with:

Inverter, Gain, $K_r = 0{,}65 \dfrac{V_{dc}}{V_{cm}} = 0{,}65 \dfrac{500}{10} = 32{,}5$

Time constant, $T_r = \dfrac{1}{2 f_c} = \dfrac{1}{2.2000} = 0{,}00025$

TABLE I
PMSM Data Parameters

Parameter	Value
Maximal Voltage	300V
Nominal Torque	14,2 Nm
Stator Resistance R_s	0,4578Ω
Number of pair poles p	4
Stator inductance in d-axis L_d	3,34 mH
Stator inductance in d-axis L_q	3,58 mH
The moment of inertia J	0,001469 *kg.m²*.*sec*
Coefficient of friction viscous B	0,0003035 Nm/Rad/sec
Flux of linkage λ_{af}	0,171 wb

$$\Rightarrow G_r(s) = \frac{K_r}{1 + sT_r} = \frac{32{,}5}{(1 + 0{,}00025s)} \tag{73}$$

$\Rightarrow$ Motor (*electrical*): *Gain,*

$\Rightarrow K_a = 1/R_s = 1/0{,}4578 = 2{,}1844$;

$\Rightarrow$ *Time constant,*

$\Rightarrow T_a = L_q / R_s = 0{,}00358 / 0{,}4578 = 0{,}0078$ sec

$$\Rightarrow G_a(s) = \frac{K_a}{1 + sT_a} = \frac{2{,}1844}{1 + s0{,}0078} \tag{74}$$

Loop induksi emf: *Torque constant,*

$$\Rightarrow K_t = \frac{3}{2}\left(\frac{p}{2}\right)^2 .\lambda_{af} = \frac{3}{2}\left(\frac{4}{2}\right)^2 .0{,}171 = 1{,}0260$$

Mechanical gain,

$$K_m = \frac{1}{B_t} = 0{,}003294 rad / \text{sec} / N.m$$

$$\Rightarrow T_m \frac{J}{B_t} = \frac{0.001469}{0.0003035} = 4{,}8402$$

$$\Rightarrow G_b(s) = \frac{K_t K_m \lambda_{af}}{(1 + sT_m)} = \frac{578.0758}{1 + s4.8402} \tag{75}$$

Motor (mechanical);

$$\Rightarrow G_m(s) = \frac{K_m K_t}{(1 + sT_m)} = \frac{0{,}003294.1.0260}{1 + s4{,}8402} = \frac{0{,}00338}{1 + s4{,}8402}$$

If, $\Rightarrow a = T_m T_{ar} = 4{,}8402.0{,}0081 = 0{,}0391$

$\Rightarrow b = T_m + K_a K_r T_m H_c = 279.7313$

$\Rightarrow K_b = K_t K_m \lambda_{af} = 1.0260 \times 0{,}003294 \times 0{,}171 = 578.0758$

$\Rightarrow c = K_a K_b = 2{,}1844 \times 578{,}0758 = 0{,}001263$, and

$\Rightarrow as^2 + bs + c = 0; \Rightarrow 0{,}0391s^2 + 279{,}7313s + 0{,}001263 = 0$

Then for the roots of the quadratic equation for a, b, and c is $\Rightarrow s_{(1,2)} = (-7154{,}3; -4.5045)$, so for value

$T_1 = 1/7154 = 0{,}0001397$;and

$T_2 = 1/4{,}5045 = 0{,}2222$

$$K_i = \frac{T_m K_r}{T_2 K_b} = \frac{4.8402 \times 32{,}5}{0{,}2222 \times 578.0758} = 1{,}2247 \ ;$$

$T_i = T_1 = 0{,}0001397$;

$$G_{is}(s) = \frac{K_i}{1 + sT_i} = \frac{1{,}2247}{1 + s0{,}0001397}$$

$$\Rightarrow \frac{y(s)}{u(s)} = \frac{K_i}{1 + sT_i} \times \frac{K_m K_t}{1 + sT_m} = \frac{0{,}00338}{1 + s4{,}8402} \times \frac{1{,}2247}{1 + s0{,}0001397}$$

$$\frac{y(s)}{u(s)}=\frac{6{,}122e06}{s^2+7157s+1479} \tag{76}$$

$$\Rightarrow s^2y+7157sy+1479y=6{,}122e06$$

$$\Rightarrow \ddot{y}+7157\dot{y}+1479y=6{,}122e06u$$

if $x_1=y\rightarrow\dot{x}_1=\dot{y}=x_2;\,x_2=\dot{y}\rightarrow\dot{x}_2=\ddot{y}$ then

$$\Rightarrow \ddot{y}=-7157\dot{y}-1479y+6{,}122e06u$$

$$\Rightarrow \dot{x}_2=-7157x_2-1479x_1+6{,}122e06u$$

$$\Rightarrow \dot{x}=\begin{bmatrix}0 & 1\\ -1479 & -7157\end{bmatrix}x+\begin{bmatrix}0\\ 6{,}122e06\end{bmatrix}u \tag{77}$$

$$\Rightarrow y=\begin{bmatrix}1 & 0\end{bmatrix}x$$

So that

$$A=\begin{bmatrix}-7157 & -1479\\ 1 & 0\end{bmatrix};B=\begin{bmatrix}1\\ 0\end{bmatrix};C=\begin{bmatrix}0 & 6{,}122e06\end{bmatrix}$$

B. Calculating Observer Gain Parameters

To design an observer controller, the first step is to determine a settling time value of 0.5 seconds with a damping ratio (ξ) value of 0.707. With the values of these parameters, a response frequency (ωn) value of $20\pm j14{,}32$ rad/sec will be obtained. The frequency response value can also be seen from the root locus analysis as shown in Figure 6.

$$q_{desired}=(s+20+14{,}32j)(s+20-14{,}32j)$$
$$=s^2+40s+605{,}0624 \tag{78}$$

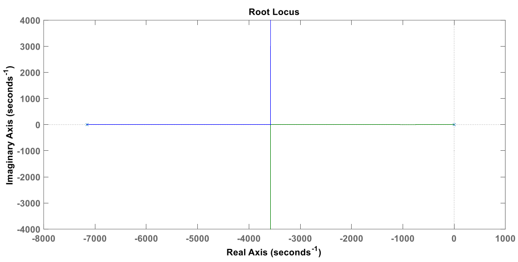

Figure 6. *Root locus* analysis

$$\Rightarrow BK=\begin{bmatrix}1\\ 0\end{bmatrix}\begin{bmatrix}K_1 & K_2\end{bmatrix}=\begin{bmatrix}K_1 & K_2\\ 0 & 0\end{bmatrix}$$

$$\Rightarrow A-BK=\begin{bmatrix}-7157 & -1479\\ 1 & 0\end{bmatrix}-\begin{bmatrix}K_1 & K_2\\ 0 & 0\end{bmatrix}=\begin{bmatrix}-7157-K_1 & -1479-K_2\\ 1 & 0\end{bmatrix}$$

$$\Rightarrow \overset{\propto}{A}=\begin{bmatrix}-7157-K_1 & -1479-K_2\\ 1 & 0\end{bmatrix}$$

$$\Rightarrow SI-\overset{\propto}{A}=\begin{bmatrix}s & 0\\ 0 & s\end{bmatrix}-\begin{bmatrix}-7157-K_1 & -1479-K_2\\ 1 & 0\end{bmatrix}$$
$$=\begin{bmatrix}s+7157+K_1 & 1479+K_2\\ -1 & s\end{bmatrix}$$

$$\Rightarrow \det\left(sI-\overset{\propto}{A}\right)=s^2+7157s+K_1s+1479+K_2$$
$$=s^2+s(7157+K_1)+1479+K_2 \tag{79}$$

Then by combining equations (78) and (79),

$$\Rightarrow 1479+K_2=605{,}0624;K_2=-873{,}9376$$

$$\Rightarrow 7157+K_1=40;K_1=-7117$$

So the value is obtained $K=\begin{bmatrix}-7117 & -873{,}938\end{bmatrix}$

To calculate value K_e, then the value must be determined first

$$A_{observer}=A^T=\begin{bmatrix}-7157 & 1\\ -1479 & 0\end{bmatrix};B_{observer}=\begin{bmatrix}0\\ 6{,}122e06\end{bmatrix};C_{observer}=\begin{bmatrix}1 & 0\end{bmatrix}$$

$$\Rightarrow L=\begin{bmatrix}L_1\\ L_2\end{bmatrix}=L.C_{observer}=\begin{bmatrix}L_1\\ L_2\end{bmatrix}\begin{bmatrix}1 & 0\end{bmatrix}=\begin{bmatrix}L_1 & 0\\ L_2 & 0\end{bmatrix}$$

$$\Rightarrow A_{observer}-L.C_{observer}=\begin{bmatrix}-7157 & 1\\ -1479 & 0\end{bmatrix}-\begin{bmatrix}L_1 & 0\\ L_2 & 0\end{bmatrix}=\begin{bmatrix}-7157-L_1 & 1\\ -1479-L_2 & 0\end{bmatrix}$$

$$\Rightarrow sI-\overset{\propto}{A}_o=\begin{bmatrix}s & 0\\ 0 & s\end{bmatrix}-\begin{bmatrix}-7157-L_1 & 1\\ -1479-L_2 & 0\end{bmatrix}=\begin{bmatrix}s+7157+L_1 & -1\\ 1479+L_2 & s\end{bmatrix}$$

$$\Rightarrow \det\left(sI-\overset{\propto}{A}_o\right)=s^2+7157s+L_1s+1479+L_2$$
$$=s^2+s(7157+L_1)+1479+L_2 \tag{80}$$

If $s1{,}2=(s+100+14{,}32j)(s+100+14{,}32j)$

$$=s^2+200s+10205{,}0624 \tag{81}$$

And by combining equations (80) and (81) we get $1479+L_2=10205{,}0624;L_2=8726.0624$ and

$$7157+L_1=200;L_1=-6957;K_e=\begin{bmatrix}L_1\\ L_2\end{bmatrix}=\begin{bmatrix}8726{,}0624\\ -6957\end{bmatrix}$$

C. Calculating LQG Gain Parameters

If $Q=\begin{bmatrix}1 & 0\\ 0 & 2\end{bmatrix};R=[1]$, then by using equations (50) and (58), the reduction to the Riccati equation [9] becomes

$$\begin{bmatrix}\dot{x}_1\\ \dot{x}_2\end{bmatrix}=\begin{bmatrix}-7157 & -1479\\ 1 & 0\end{bmatrix}\begin{bmatrix}x_1\\ x_2\end{bmatrix}+\begin{bmatrix}0\\ 6{,}122e06\end{bmatrix}u$$

$$y=\begin{bmatrix}1 & 0\end{bmatrix}x$$

$$J=\int_0^\infty\left[x^T\begin{bmatrix}2 & 0\\ 0 & 1\end{bmatrix}x+u^2\right]dt$$

and $PA+A^TP+Q-PBR^{-1}B^TP=0$.

$$\Rightarrow PA=\begin{bmatrix}p_{11} & p_{12}\\ p_{21} & p_{22}\end{bmatrix}\begin{bmatrix}-7157 & -1479\\ 1 & 0\end{bmatrix}=\begin{bmatrix}-7157p_{11}+p_{12} & -1479p_{11}\\ -7157p_{21}+p_{22} & -1479p_{21}\end{bmatrix}$$

$$\Rightarrow A^T=\begin{bmatrix}-7157 & 1\\ -1479 & 0\end{bmatrix}\text{so that}$$

$$\Rightarrow A^TP=\begin{bmatrix}-7157 & 1\\ -1479 & 0\end{bmatrix}\begin{bmatrix}p_{11} & p_{12}\\ p_{21} & p_{22}\end{bmatrix}=\begin{bmatrix}-7157p_{11}+p_{21} & -7157p_{12}+p_{22}\\ -1479p_{11} & -1479p_{12}\end{bmatrix}$$

$$\Rightarrow PBR^{-1}B^TP=\begin{bmatrix}p_{11} & p_{12}\\ p_{21} & p_{22}\end{bmatrix}.\begin{bmatrix}1\\ 0\end{bmatrix}.1.\begin{bmatrix}1 & 0\end{bmatrix}.\begin{bmatrix}p_{11} & p_{12}\\ p_{21} & p_{22}\end{bmatrix}$$

$$\Rightarrow PBR^{-1}B^TP=\begin{bmatrix}p_{11}\\ p_{21}\end{bmatrix}\begin{bmatrix}p_{11} & p_{12}\end{bmatrix}=\begin{bmatrix}p_{11}p_{11} & p_{11}p_{12}\\ p_{21}p_{11} & p_{21}p_{12}\end{bmatrix}$$

$$\Rightarrow PA+A^TP+Q-PBR^{-1}B^TP=0$$

$$\Rightarrow\begin{bmatrix}-7157p_{11}+p_{12} & -1479p_{11}\\ -7157p_{21}+p_{22} & -1479p_{21}\end{bmatrix}+\begin{bmatrix}-7157p_{11}+p_{21} & -7157p_{12}+p_{22}\\ -1479p_{11} & -1479p_{12}\end{bmatrix}+$$
$$\begin{bmatrix}1 & 0\\ 0 & 2\end{bmatrix}-\begin{bmatrix}p_{11}p_{11} & p_{11}p_{12}\\ p_{21}p_{11} & p_{21}p_{12}\end{bmatrix}=0 \tag{82}$$

If the matrix P is a symmetric matrix, then $p_{12}=p_{21}$

$$\Rightarrow\begin{bmatrix}-14314p_{11}+2p_{12} & -1479p_{11}-7157p_{12}+p_{22}\\ -1479p_{11}-7157p_{12}+p_{22} & -2958p_{21}\end{bmatrix}+$$
$$\begin{bmatrix}1-p_{11}^2 & -p_{11}+p_{12}\\ -p_{12}p_{11} & 2-p_{12}^2\end{bmatrix}=0$$

then the P matrix is obtained:

$$P=\begin{bmatrix}14314 & 2958\\ 2958 & 42340812\end{bmatrix}$$

And by using equation (55),

$$K_r = R^{-1}B^T P = \begin{bmatrix}1 & 0\end{bmatrix}\begin{bmatrix}14314 & 2958 \\ 2958 & 42340812\end{bmatrix} = \begin{bmatrix}1434 & 2958\end{bmatrix}$$

D. Performing Tests and Analysis When the Motor is Without Load

For the course of research, the motor will rotate clockwise (CW) with no load. A few moments later a 5 Nm load is added to the system so that the motor is under load, and then the rotor rotation is reversed according to the counter clock wise (CCW) direction. The CW and CCW directions indicate that the motor is serving hydraulic loads with extension and retraction. The analysis carried out in this study is the parameters of the rotor rotation speed, the parameters of the electric power torque, and the parameters of the q-axis stator current.

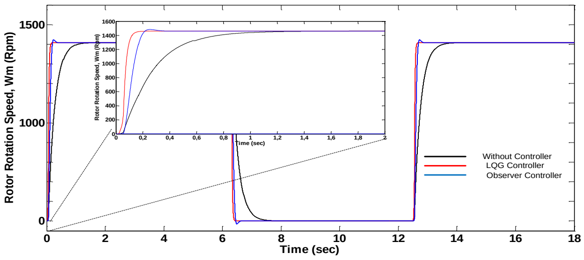

Figure 7. Rotor speed response at no load

TABLE II
EXPERIMENTAL DATA OF ROTOR SPEED AT NO LOAD

Rotor Rotation Speed (rad/sec)	Rise Time (sec)	Settling Time (sec)	Steady State Value (rad/sec)
Without Controller	0,475	1,58	181,7
Observer Controller	0,123	0,34	181,7
LQG Controller	0,055	0,165	181,7

In Figure 7, the time required for the rotor rotation speed with observer control to reach settling time is 0.34 seconds, which is 364.705% faster than the rotor rotation speed without controllers which reaches 1.58 seconds. Meanwhile, the time required for the rotor rotation speed with the LQG controller during the settling time reached 0.165 seconds, which was 106.061% faster than the rotor rotation speed with the observer controller which reached 0.34 seconds. For the value of the rotor rotation speed at steady state, the value is the same among the three, namely 181.7 rad/sec.

In Figure 8, the time required by the electric power torque with observer control to reach settling time is 0.39 seconds, which is 248.72% faster than the time required by the electric power torque without controller which reaches 1, 36 seconds. While the time needed by the electric power torque with the LQG controller to reach the settling time is 0.18 seconds, which is 116.67% faster than the time needed by the electric power torque with the observer controller which reaches 0, 39 seconds. For the magnitude of the electric power torque value at steady state is the same value among the three, namely 0.4431 Nm.

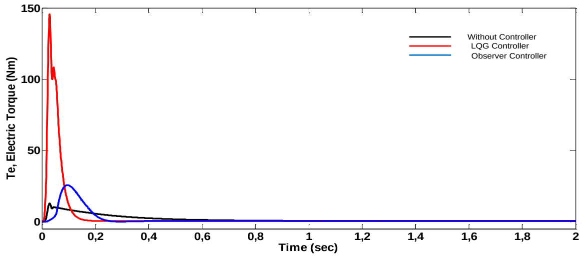

Figure 8. Response of electric power torque at no load

TABLE III
ELECTRICAL POWER TORQUE EXPERIMENTAL DATA AT NO LOAD

Te, Elektrik Torque (Nm)	Peak Torque (Nm)	Settling Time (sec)	Steady State Value (Nm)
Without Controller	12,9	1,36	0,4431
Observer Controller	25,7	0,39	0,4431
LQG Controller	145,6	0,18	0,4431

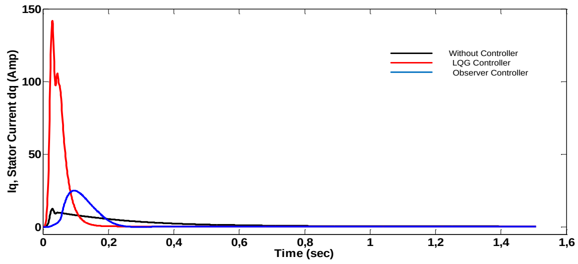

Figure 9. Q-axis stator current response at no-load

TABLE IV
EXPERIMENTAL DATA OF THE Q-AXIS STATOR CURRENT AT NO LOAD

Iq, dq, Current Stator (Amp)	Peak Current (Amp)	Settling Time (sec)	Steady State Value (Amp)
Without Controller	12,58	1,36	0,4339
Observer Controller	25,04	0,39	0,4319
LQG Controller	141,9	0,18	0,4319

In Figure 9, the time required for the q-axis stator current with an observer controller to reach settling time is 0.39 seconds, which is 248.72% faster than the time required for the q-axis stator current without a controller. which reached 1.36 seconds. Meanwhile, the time required by the q-axis stator current with the LQG controller to achieve settling time is 0.18 seconds, which is 116.67% faster than the time required by the q-axis stator current with the observer controller which reaches 0.39 sec. For the magnitude of the value of the stator current on the q-axis when the steady state state is of the same value among the three, which is equal to 0.432 Amperes.

E. Performing Tests and Analysis When the Motor is Loaded

Further testing of the motor with a load is the addition of a load of 5 Nm. Speed reference starts from 1446.65 rpm at steady state. In Figure 10, the time required for the rotor rotation speed with observer control to reach settling time is 0.34 seconds, which is 364.705% faster than the rotor rotation speed without controllers which reaches 1.58 seconds. Meanwhile, the time required for the rotor rotation speed with the LQG controller during the settling time reached 0.165 seconds, which was 106.061% faster than the rotor rotation speed with the observer controller which reached 0.34 seconds. For the value of the rotor rotation speed at steady state, the observer controller is 74.49% greater than without the controller, and the rotor rotation speed with the LQG controller is 8.29% greater than the observer controller, which is 1397 Rpm.

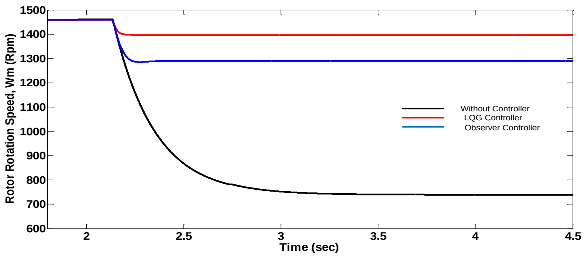

Figure 10. Response of rotor speed when loaded

TABLE V
EXPERIMENTAL DATA OF ROTOR SPEED UNDER LOAD

Rotor Rotation Speed (Rpm)	Down Time (sec)	Settling Time (sec)	Steady State Value (Rpm)
Without Controller	0,24	1,26	739,3
Observer Controller	0,05	0,26	1290
LQG Controller	0,015	0,12	1397

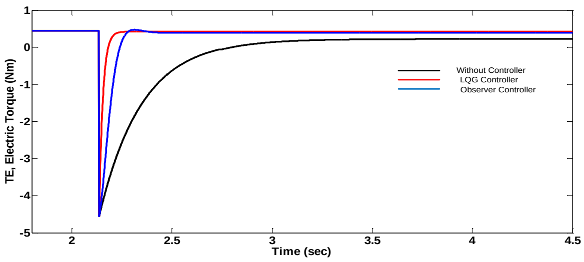

Figure 11. Response of electric power torque at load

TABLE VI
EXPERIMENTAL DATA OF ELECTRIC POWER TORQUE AT LOAD

Te, Elektrik Torque (Nm)	Peak Torque (Nm)	Settling Time (sec)	Steady State Value (Nm)
Without Controller	4,94	1,18	10,22
Observer Controller	4,94	0,26	10,39
LQG Controller	4,94	0,11	10,42

In Figure 11, the time needed by the electric power torque with observer control to reach settling time is 0.26 seconds, which is 353.85% faster than the time needed by the electric power torque without controller which reaches 1, 18 seconds. Meanwhile, the time needed by the electric power torque with the LQG controller to reach the settling time is 0.11 seconds, which is 136.36% faster than the time needed by the electric power torque with the observer controller which is 0.26 seconds. . For the value of the electric power torque at steady state, the observer controller is 1.66% greater than without the controller, and the electric power torque with the LQG controller is 0.29% greater than the observer controller.

In Figure 12, the time required by the q-axis stator current with an observer controller to reach settling time is 0.27 seconds, which is 366.67% faster than the time required by the q-axis stator current without a controller which reached 1.26 seconds. While the time required by the q-axis stator current with the LQG controller to reach settling time is 0.104 seconds, which is 159.62% faster than the time required by the q-axis stator current with the observer controller which reaches 0, 27 seconds. For the value of the stator current on the q-axis at steady state, the observer controller is 3.21% greater than without a controller, and the value of the stator current on the q-axis with the LQG controller is 0.599% greater than that of the observer controller.

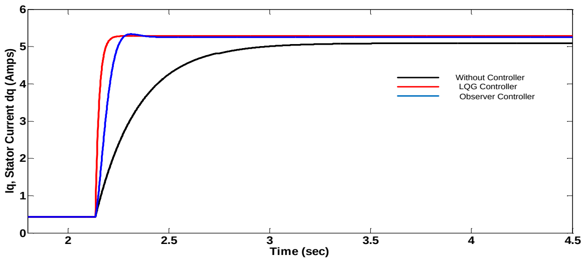

Figure 12. Q-axis stator current response when loaded

TABLE VII
EXPERIMENTAL DATA OF THE Q-AXIS STATOR CURRENT AT LOAD

Iq, dq Stator Current (Amp)	Rise Time (sec)	Settling Time (sec)	Steady State Value (Amp)
Without Controller	0,6	1,26	5,092
Observer Controller	0,092	0,27	5,255
LQG Controller	0,033	0,104	5,286

F. Performing Tests and Analysis When the Motor Reverses Direction

The next motor test is in a reversed position but still under a load of 5 Nm. Speed reference starts with the steady state of each system. In Figure 13, the time required for the rotor rotation speed with observer control to reach settling time is 0.44 seconds, which is 213.64% faster than the rotor rotation speed without controllers which reaches 1.38 seconds. Meanwhile, the time required for the rotor rotation speed with the LQG controller during the settling time reaches 0.2 seconds, which is 120% faster than the rotor rotation speed with

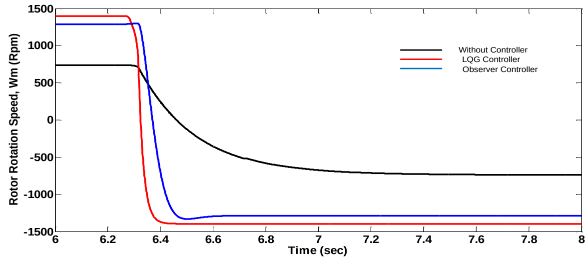

Figure 13. Response of rotor speed when the motor reverses

TABLE VIII
ROTOR SPEED DATA WHEN THE MOTOR IS REVERSING

Rotor Rotation Speed (Rpm)	Rise Time (sec)	Settling Time (sec)	Steady State Value (Rpm)
Without Controller	0,37	1,38	-739,3
Observer Controller	0,115	0,44	-1290
LQG Controller	0,05	0,2	-1397

the observer controller which reaches 0.44 seconds. For the value of the rotor rotation speed at steady state, the observer controller is 74.49% greater than without the controller, and the rotor rotation speed with the LQG controller is 8.29% greater than the observer controller, which is 1397 Rpm.

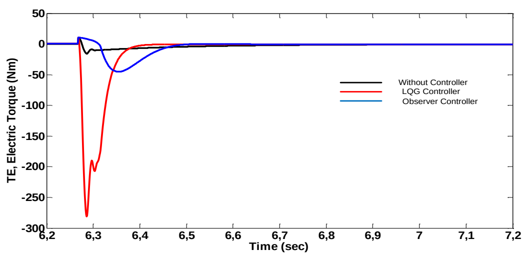

Figure 14. Response of electric power torque when the motor reverses

TABLE IX
ELECTRICAL POWER TORQUE DATA WHEN THE MOTOR REVERSES DIRECTION

Te, Elektrik Torque (Nm)	Peak Torque (Nm)	Settling Time (sec)	Steady State Value (Nm)
Without Controller	-15,6	1,28	-0,2244
Observer Controller	-45,18	0,36	-0,3915
LQG Controller	-281,2	0,16	-0,4238

In Figure 14, the time required by the electric power torque with observer control to reach settling time is 0.36 seconds, which is 255.56% faster than the time required by the electric power torque without controller which reaches 1, 28 seconds. Meanwhile, the time needed by the electric power torque with the LQG controller to reach the settling time is 0.16 seconds, which is 125% faster than the time needed by the q-axis stator current with the observer controller which is 0.36 seconds. . For the value of the electric power torque at steady state, the observer controller is 74.47% greater than without the controller, and the electric power torque with the LQG controller is 8.25% greater than the observer controller, which is 0.4238 Nm.

In Figure 15, the time required for the q-axis stator current with an observer controller to reach settling time is 0.37 seconds, which is 272.97% faster than the time required for the q-axis stator current without a controller. which reached 1.38 seconds. While the time required by the q-axis stator current with the LQG controller to reach settling time is 0.16 seconds, which is 131.25% faster than the time required by the q-axis

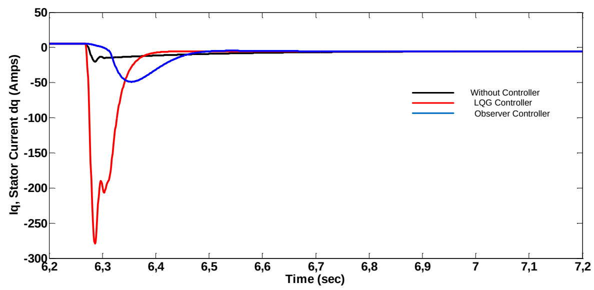

Figure 15. Q-axis stator current response when the motor reverses

TABLE X
Q-AXIS STATOR CURRENT DATA WHEN THE MOTOR IS REVERSING

Iq, Stator Current dq (Amp)	Peak Current (Amp)	Settling Time (sec)	Steady State Value (Amp)
Without Controller	-20,07	1,38	-5,092
Observer Controller	-48,92	0,37	-5,286
LQG Controller	-278,86	0,16	-5,255

stator current with the observer controller which reaches 0.37 sec. For the magnitude of the value of the stator current on the q-axis when the steady state is the observer controller is 3.2% greater than without a controller, and the stator current on the q-axis with the LQG controller is 0.59% greater than the observer controller which is 5.255 amperes.

V. CONCLUSION

From the results of research on the characteristics of PMSM applied in hydraulic systems, it can be seen that the LQG controller is more optimal when compared to the observer controller. The more optimal referred to in this study is the transient response which is faster, which is indicated by the improvement in the settling time value at no load, namely 116.67% for the observer controller and 364.705% without the controller.

Then when the synchronous motor serves the nominal load, the rotational speed of the rotor produced in steady state becomes 8.29% faster than the observer controller and 74.49% without the controller. The rotational speed of this rotor affects the time needed by the actuator to extend and retract.

REFERENCES

[1] Lee, W., Li, S., Han, D., Sarlioglu, B., Minav, T. A., & Pietola, M. (2017, September). Achieving high-performance electrified actuation system with integrated motor drive and wide bandgap power electronics. In *2017 19th European Conference on Power Electronics and Applications (EPE'17 ECCE Europe)* (pp. P-1). IEEE.

[2] Zakharov, V., & Minav, T. (2023). Analysis of Frequency adjustable control of Permanent Magnet Synchronous Motor for pump-controlled actuators. *International Journal of Fluid Power*, 125-140.

[3] Minav, T. A., Pyrhonen, J. J., & Laurila, L. I. (2011). Permanent magnet synchronous machine sizing: effect on the energy efficiency of an electro-hydraulic forklift. *IEEE Transactions on Industrial Electronics*, *59*(6), 2466-2474.

[4] Mitov, A., Slavov, T., Kralev, J., & Angelov, I. (2019, July). Comparison of robust stability for electrohydraulic steering control system based on LQG and H-infinity controller. In *2019 42nd International Conference on Telecommunications and Signal Processing (TSP)* (pp. 712-715). IEEE.

[5] Molavi, R., Shojaee, K., & Khaburi, D. A. (2008, December). Optimal vector control of permanent magnet synchronous motor. In *2008 IEEE 2nd International Power and Energy Conference* (pp. 249-253). IEEE.

[6] Alfehaid, A. A., Strangas, E. G., & Khalil, H. K. (2020). Speed control of permanent magnet synchronous motor with uncertain parameters and unknown disturbance. *IEEE Transactions on Control Systems Technology*, *29*(6), 2639-2646.

[7] Krishnan, R. (2001). *Electric motor drives: modeling, analysis, and control*. Pearson.

[8] Krishnan, R. (2017). *Permanent magnet synchronous and brushless DC motor drives*. CRC press.

[9] Burns, R. (2001). *Advanced control engineering*. Elsevier.

[10] Skogestad, S., & Postlethwaite, I. (2005). *Multivariable feedback control: analysis and design*. john Wiley & sons.

[11] Zhou, K., & Doyle, J. C. (1998). *Essentials of robust control* (Vol. 104). Upper Saddle River, NJ: Prentice hall.

[12] LLagrioui, A., & Mahmoudi, H. (2011, April). Speed and current control for the PMSM using a Luenberger observer. In *2011 International Conference on Multimedia Computing and Systems* (pp. 1-6). IEEE.

[13] Mitov, A., Kralev, J., Slavov, T., & Angelov, I. (2020, June). Real-Time LQG Control Strategies for Electrohydraulic Steering of Mobile Machines. In *2020 21st International Symposium on Electrical Apparatus & Technologies (SIELA)* (pp. 1-4). IEEE.

[14] Mitov, A., Slavov, T., Kralev, J., & Angelov, I. (2018, July). H-infinity Control of an Electrohydraulic Power Steering System. In *2018 41st International Conference on Telecommunications and Signal Processing (TSP)* (pp. 1-4). IEEE.

[15] Zheng, D., & Xu, H. (2017, May). Robust H∞ control of a friction based electrohydraulic load simulator. In *2017 29th Chinese Control And Decision Conference (CCDC)* (pp. 3961-3966). IEEE.

[16] Nicolae, V., Toma, C. G., Constantin, C., Daniela, V., & Daniel, B. M. (2018, May). Modeling and simulation of a hybrid electrohydraulic flight control servomechanism for a380. In *2018 7th International Conference on Computers Communications and Control (ICCCC)* (pp. 150-155). IEEE.

[17] Lee, J. C., Misawa, E. A., & Reid, K. N. (1996, September). Stability robustness applied to the design of electrohydraulic servovalve. In *Proceeding of the 1996 IEEE International Conference on Control Applications IEEE International Conference on Control Applications held together with IEEE International Symposium on Intelligent Contro* (pp. 534-539). IEEE

[18] Yordanov, S., Ormandzhiev, K., Mihalev, G., & Kostov, K. (2020, October). Identification and synthesis of PI controller for electrohydraulic servo system. In *2020 International Conference Automatics and Informatics (ICAI)* (pp. 1-5). IEEE.

[19] Deng, Z., & Nian, X. (2015). Robust control of permanent magnet synchronous motors. *IEEE/CAA Journal of Automatica Sinica*, *2*(2), 143-150.

[20] Mendoza-Mondragón, F., Hernández-Guzmán, V. M., & Rodríguez-Reséndiz, J. (2018). Robust speed control of permanent magnet synchronous motors using two-degrees-of-freedom control. *IEEE Transactions on Industrial Electronics*, *65*(8), 6099-6108.

[21] Mun-Soo, K., Song, D. S., Lee, Y. K., Won, T. H., Park, H. W., Jung, Y. I., ... & Lee, H. (2001, June). A robust control of permanent magnet synchronous motor using load torque estimation. In *ISIE 2001. 2001 IEEE International Symposium on Industrial Electronics Proceedings (Cat. No. 01TH8570)* (Vol. 2, pp. 1157-1162). IEEE.

[22] Li, L., Pei, G., Liu, J., Du, P., Pei, L., & Zhong, C. (2020). 2-DOF Robust $ H_ {\infty} $ Control for Permanent Magnet Synchronous Motor With Disturbance Observer. *IEEE Transactions on Power Electronics*, *36*(3), 3462-3472.

[23] Zhao, G., Chen, S., Liu, Y., & Guo, K. (2022). A Novel Reference Governor for Disturbance Observer-Based Load Pressure Control in a Dual-Actuator-Driven Electrohydraulic Actuator. *Applied Sciences*, *12*(16), 8367.

[24] Rybarczyk, D., & Milecki, A. (2020). Electrohydraulic Drive with a Flow Valve Controlled by a Permanent Magnet Synchronous Motor. *Transactions of FAMENA*, *44*(2), 31-44.

[25] Xuan, W., & Fanquan, Z. (2018). Design of electro-hydraulic servo loading controlling system based on fuzzy intelligent water drop fusion algorithm. *Computers & Electrical Engineering*, *71*, 485-491.

[26] Zhang, H., & Quan, L. (2010, August). Permanent magnet synchronous motor servo system with adaptive observer. In *2010 International Conference on Computer, Mechatronics, Control and Electronic Engineering* (Vol. 3, pp. 120-123). IEEE.

[27] Zhang, C. C., & Jiang, Z. F. (2014). Simulation study of permanent magnet synchronous motor for hydraulic electromagnetic energy-regenerative shock absorber. In *Applied Mechanics and Materials* (Vol. 530, pp. 1011-1014). Trans Tech Publications Ltd.

[28] Liu, C., & Jiang, H. (2014). A seventh-order model for dynamic response of an electro-hydraulic servo valve. *Chinese Journal of Aeronautics*, *27*(6), 1605-1611.

[29] Othman, S. M., Rahmat, M. F., Rozali, S. M., & Salleh, S. (2015). Review on sliding mode control and its application in electrohydraulic actuator system. *Journal of Theoretical and Applied Information Technology*, *77*(2), 199-208.

[30] Daode, Z., Pian, Y., Zhouxing, W., & Yuan, W. (2017). Study on Electro-hydraulic Servo Valve Control System of Series Manipulator. *International Journal of Control and Automation*, *10*(3), 289-302.

[31] Hasan, J., Karmaker, T., & Ahmed, M. I. (2019). Mathematical Modeling and Simulation based System Identification of Non-Minimum Phase Electro-Hydraulic Servo (EHS) System. *International Journal of Engineering Research & Technology (IJERT)*, *8*(9), 189-195.

[32] Ahmed, M. I., & Azad, A. K. M. (2016, November). Mathematical modeling and DLQR based controller design for a non-minimum phase Electro Hydraulic Servo system (EHS). In *2016 IEEE Region 10 Conference (TENCON)* (pp. 1839-1844). IEEE.

[33] Lee, J. C., Misawa, E. A., & Reid, K. N. (1996, September). Stability robustness applied to the design of electrohydraulic servovalve. In *Proceeding of the 1996 IEEE International Conference on Control Applications IEEE International Conference on Control Applications held together with IEEE International Symposium on Intelligent Contro* (pp. 534-539). IEEE.

[34] Zheng, D., & Xu, H. (2017, May). Robust H∞ control of a friction based electrohydraulic load simulator. In *2017 29th Chinese Control And Decision Conference (CCDC)* (pp. 3961-3966). IEEE.

[35] Ming, X., & Bo, J. (2012, June). Step-response simulation of energy regulation based electrohydraulic variable-speed drive. In *2012 IEEE International Conference on Information and Automation* (pp. 40-44). IEEE.

[36] Lim, T. J. (1997, May). Pole placement control of an electrohydraulic servo motor. In *Proceedings of Second*

International Conference on Power Electronics and Drive Systems (Vol. 1, pp. 350-356). IEEE.
[37] Deng, W., & Yao, J. (2019). Extended-state-observer-based adaptive control of electrohydraulic servomechanisms without velocity measurement. *IEEE/ASME Transactions on Mechatronics*, *25*(3), 1151-1161.
[38] Won, D., Kim, W., & Tomizuka, M. (2017). High-gain-observer-based integral sliding mode control for position tracking of electrohydraulic servo systems. *IEEE/ASME transactions on mechatronics*, *22*(6), 2695-2704.

NOMENCLATURE

i_{ds}^r, i_{qs}^r Steady-state stator q- and d-axes currents in rotor reference frames, Ampere

v_{qs}^r Stator voltage vector in rotor reference frames, Volts

R_s *Stator resistance per phase*, Ω

L_q, L_d Quadrature and direct axis stator self-inductances in rotor reference frames, Henry

ω_r *Speed reference*

λ_{af} Armature flux linkages due to rotor magnets at ambient temperature, V-s

T_e *Air gap or electromagnetic torque*, Nm

T_l *Load torque*, Nm

J *Total moment of inertia*, $kg-m^2$

p *Number of poles*

B_1 *Friction coefficient*, Nm/(rad/s)

B_t *Total friction coefficient*, Nm/(rad/s)

K_t *Torque constant*, Nm/A

K_r *Inverter gain*, V/V

K_a *Inverse of leakage factor*

K_b *Induced emf constant*, V/(rad/s)

K_m Ratio between mutual and self-inductances

K_i Current loop transfer function gain

T_a Carrier period time, s, as well as effective turns per stator phase winding

T_i *Time lag of the current control loop*, s

T_m *Mechanical time constant*, s

T_r *Converter (inverter) time delay*, s

T_ω *Time constant of the speed filter*, s

T_1, T_2 Electrical time constants of the motor, s

f_c Control frequency, and PWM carrier frequency, Hz

e_a *Induced emf in phase a* (*instantaneous*), V

H_ω *Gain of the speed filter*, V/(rad/s)